

## Inner circumference measurement with point autofocus probe

Katsuhiro Miura<sup>1\*</sup>, Atsuko Nose<sup>1</sup>, Takao Tsukamoto<sup>1</sup>

<sup>1</sup>1-18-8, Nozaki, Mitaka-shi, Tokyo 181-0014 Japan

[miura@mitakakohki.co.jp](mailto:miura@mitakakohki.co.jp)

### Abstract

Inner circumference measurement of complex small parts, such as watch parts, and barrels for small-lenses dedicated for smartphones, has been in a great demand in recent years. To meet this demand, a new measuring method was developed. This method tilts the laser optical axis of a point autofocus probe (PAP), applying high angle tracking ability of PAP, in order to reach to the inner circumference of the small parts. It has effective measuring inclination angles and measures cross section contour and circumference contour and 3D of a workpiece having its inner diameter less than several millimeters in sub-micron accuracy without repositioning by setting the optimal measuring conditions. In this paper, measurement accuracy and repeatability of inner circumference measurement were verified by using high magnification objective lenses. It is useful for inner circumference measurement of small lens barrels and small precision parts.

**Keywords:** Inner circumference measurement, Point autofocus probe, Barrel, Roundness, 3D form, Surface texture

### 1. Introduction

It is common to use low pressure stylus and image processing measuring instruments for measuring inner circumference of small parts. However, it is difficult for contact stylus instruments to carry out high precision measurement due to requiring long measuring time, displacing and deforming the workpiece with their contact pressure. Also, image processing measuring instruments have trouble obtaining correct inner surface image as the edge image is affected by brightness of the illumination. To solve this restriction, autofocus (AF) optical axis tilt measuring method (AFOT), tilting the AF optical axis of a point autofocus probe (PAP) to measure inner circumference, was developed. This measuring method utilizes steep angle surface tracking ability of PAP [1] to autofocus on the inner surface in a diagonal direction and measures the inner surface directly. This paper presents the new measuring method, measurement accuracy and repeatability of AFOT and shows some measurement results of small precision parts.

### 2. AF optical axis tilt measuring method

This measuring method is described in Fig. 1. The AF driving axis is in horizontal direction(X) while the AF optical axis is tilted at a fixed angle (A) for measuring the inner surface. With this setting, PAP directly measures inner diameter and roundness by rotating the workpiece in the AZ axis direction. In addition, AFOT offers contour and 3D measurements by setting the AZ axis as the stepping axis and scanning in the Z axis. Fig. 2 shows the measurement instrument for this study [2]. This instrument is equipped with 6-axis control mechanism; 4 linear motion axes and 2 rotation axes. This feature allows the AF probe to approach to a workpiece in various directions. The X, Y and Z linear motion axes are loaded with 10 nm resolution linear scales and the AF axis is loaded with 1 nm resolution linear scale. The workpiece is set on the AZ axis and the AF probe is mounted on the Z axis. This instrument was modified in order to keep the AF driving axis in a horizontal position yet the AF optical axis is

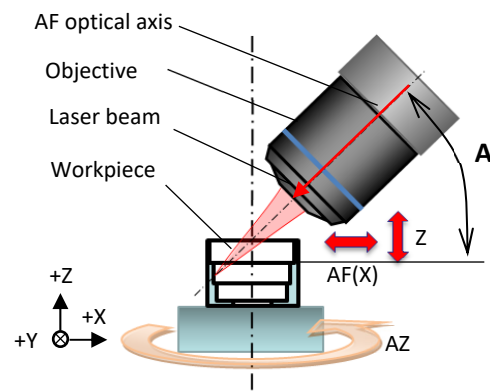


Figure 1. AF optical axis tilt measuring method

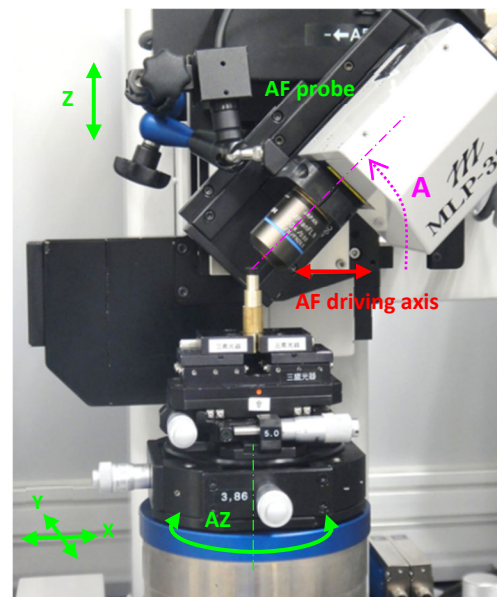


Figure 2. 3D form measuring instrument (Model: MLP-3SP)

adjustable in various angles. This modified instrument enables to measure workpieces having inner diameter and depth up to 7 mm with a 50x objective (WD = 10.6 mm) with the AF optical axis at 45°.

### 3.Verification of measurement accuracy

#### 3.1. Maximum measurable angle

The maximum measurable inclination angle that does not generate scattered light with surface roughness in nanometer level ( $A_3$ ) is given by the following equation [3]:

$$A_3 < \frac{\alpha}{2} + \frac{b}{4} \quad (1)$$

Fig. 3 shows each symbol of the laser beam path in detail. This formula gives the maximum measurable angle is  $A_3 = 25^\circ$  with 50x objective and  $A_3 = 45^\circ$  with 100x objective. However, it is possible to measure greater angle than  $A_3$  as the AF sensor captures the scattered light generated by the workpiece surface having several tens of nanometer surface roughness [4]. Fig. 4 shows a measurement result of a pin gauge having surface roughness  $Ra = 0.1 \mu\text{m}$ . This profile measurement proves that  $\pm 88^\circ$  slope is measurable.

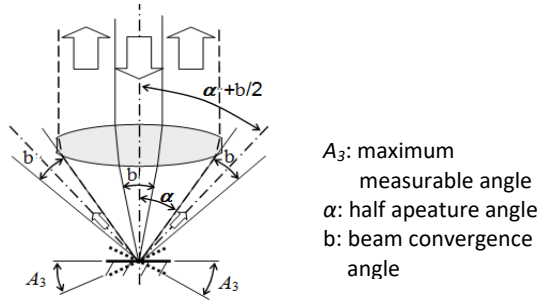


Figure 3. Maximum measurable inclination angle

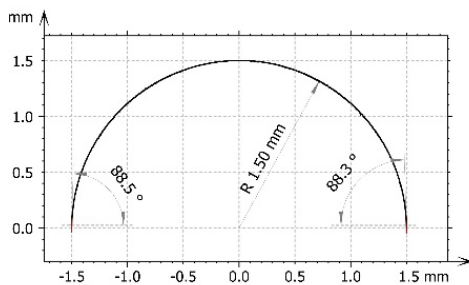


Figure 4. D=3mm pin gauge profile (50x objective)

#### 3.2. Change of surface texture parameters against inclination angle

In order to verify the measurement accuracy against inclined planes, a roughness reference material having  $Ra = 0.5 \mu\text{m}$  was measured by changing its setting angle at every  $5^\circ$  from  $0^\circ$  up to  $85^\circ$ . Fig. 5 shows the measurement result. The horizontal axis shows inclination angle and the vertical axis shows correlation against the roughness standard. Amplitude parameter value ( $Ra$ ) with the 50x objective is same as that of the reference value ranging from  $0^\circ$  to  $10^\circ$ . And,  $Ra$  increases as the angle becomes greater and reaches to its peak near the maximum measurable inclination angle ( $25^\circ$ ). It drastically decreases at  $30^\circ$  and becomes stable up to  $85^\circ$ . On the other hand, with the 100x objective, it remains the same as the reference value,  $0^\circ$ , up to  $25^\circ$  and reaches to the peak near the maximum measurable inclination angle ( $45^\circ$ ) likewise. It becomes closer to the reference value at the greater angle than  $50^\circ$ . Fig. 6 shows the roughness profile at each set angle with different objective lenses. The roughness profile at  $20^\circ$  in Fig. 6-a is approximately 7 times larger value than the reference profile at  $0^\circ$ . On the other

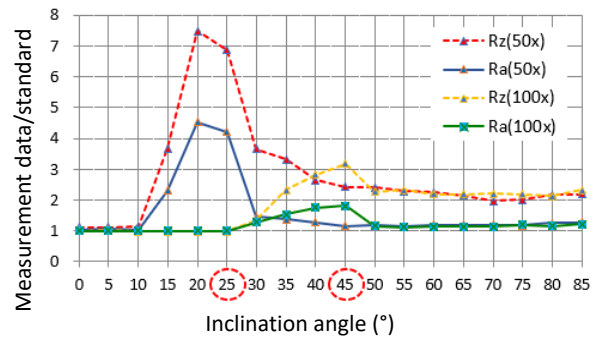


Figure 5. Change of the surface texture parameter against inclination angle

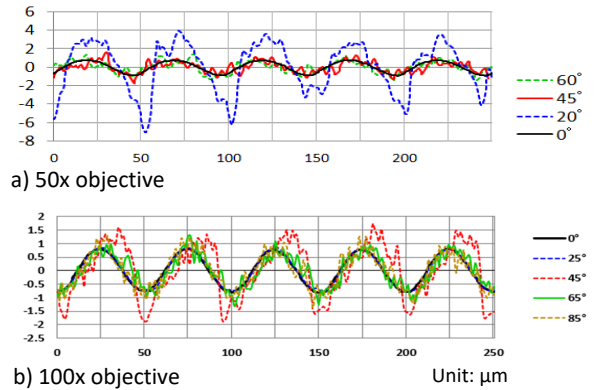


Figure 6. Comparison of roughness profile of different inclination angle

hand, the roughness profiles at  $45^\circ$  and  $60^\circ$  show closer values to the reference profile with the presence of micro-noise. Fig. 6-b shows the changes in roughness profile with the 100x objective. The roughness profile increases almost twice at  $45^\circ$ , comparing with the reference profile at  $0^\circ$ , with indication of micro noise in sub-micron level at greater inclination angle. However, it shows a similar result to the reference profile at  $0^\circ$ .

For the inclination angles from  $0^\circ$  to  $10^\circ$ , the objective captured all the reflected laser beam. For the inclination angles from  $10^\circ$  to  $25^\circ$ , the reflected laser beam was at the circumference of the objective. For over  $25^\circ$ , PAP autofocused on the workpiece surface only with the scattered light. From these results, the optimal angles of the AF optical axis for high accuracy measurement with the 50x objective are from  $0^\circ$  to  $10^\circ$  and over  $30^\circ$ , excepting for the angles where the reflected laser beam is at the circumference of the objective, and that with the 100x objective are from  $0^\circ$  to  $25^\circ$  and over  $50^\circ$ . However, as the inclination angle increases, the scattered light captured by the AF sensor decreases. This causes signal-to-noise ratio (SNR) decreases, leading the AF focusing speed to slow down. Hence, the ideal AF optical axis angles for high precision measurement of inclined planes, having sub-micron roughness that generates scattering light, are  $45^\circ$  for the 50x and  $60^\circ$  for the 100x objectives.

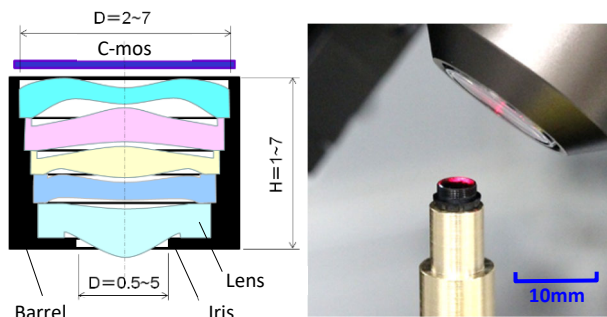
#### 3.3. Accuracy verification of roundness measurements

To verify the inner diameter measurement accuracy, 2 ring gauges were measured; one has 5.999 mm diameter (Ring A) and the other has 1.004 mm diameter (Ring B). The roundness of Ring A was measured with the 50x objective with AF optical axis tilt angle =  $45^\circ$  and that of Ring B was measured with the 100x objective with the tilt angle =  $75^\circ$ . Both ring gauges were measured 20 times, and the result shows that both PV values are less than  $0.1 \mu\text{m}$ . Also, the roundness of the ring gauges were measured by repositioning 4 times, changing phase at every  $90^\circ$  from  $0^\circ$  to  $270^\circ$ . As a result, PV values are less than  $0.2 \mu\text{m}$ .

#### 4. Inner circumference measurement of lens barrel

##### 4.1. Measurement items and required accuracy

Camera lens for smartphones consist of several aspherical lenses (Fig. 7-a). For aspherical lenses, eccentricity amount of each lens directly and greatly affects their optical performance. In order to reduce the eccentricity amount, the fitting of the inner diameter of barrel for holding these lenses and the circumference of the lenses are critical, and the gap between the barrel and the lenses must be controlled in a-few-micron level. To meet these requirements, it is very important to measure the inner circumferences of each steps. The reference lens for the optical axis is the bottom lens depicted in Fig. 7-a. It is also crucial to measure the inner corner form of the bottom and the contour of the bottom iris. Most of the barrels are made of plastic with several millimeters in size. There has been no proposal of non-contact method that carries out high precision measurement of black plastic material with low reflectivity and inner diameter having multistep part of inner rings in sub-micron level yet. AFOT is a only one non-contact measuring method that meets these requirements (Fig. 7-b).



a) Small camera lens module b) Barrel inner measurement

Figure 7. Camera lens module for smartphone

##### 4.2. Measurement example 1): Cross section contour

PAP was set as described in Fig. 1. The AZ axis is the stepping axis and the Z axis is the scanning axis. Profile measurement of a barrel was carried out as follows: scan in the Z axis from the bottom to the top of the barrel with the AZ axis at 0°, and rotate the AZ axis 180° and repeat the Z-axis scan. The obtained data was transformed to coordinates, referencing to the rotation center coordinates of the instrument, and combined them to produce a cross-section contour of the inside of the barrel. Fig. 8 shows an example of cross-section contour measurement of a barrel having less than 2-mm inner diameter. PAP measured from the edge form of the iris at the bottom up to the tip of the inner diameter at the top of the barrel.

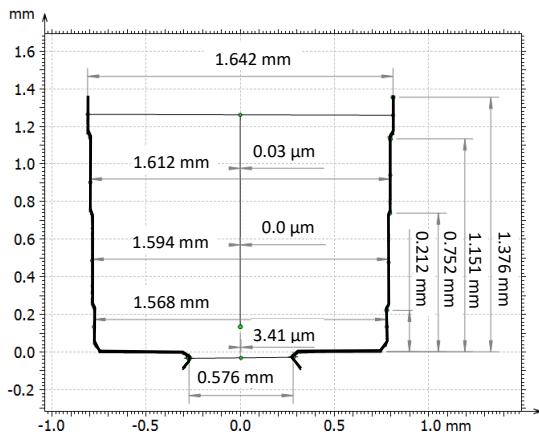


Figure 8. Barrel inner crosssection contour

##### 4.3. Measurement example 2): Circumference measurement (diameter, roundness and eccentricity measurements)

Each inner circumference of the barrel was measured by setting the Z axis as the stepping axis and the AZ axis as the scanning axis. This measurement setting is as same as that of the cross-section contour measurement in the previous subsection, yet it also offers diameter, roundness and eccentricity measurements. The circumference measurement enables to carry out high speed measurement by setting the AZ axis rotation speed at 20° per second with Scan mode [5]. The measurement time of one circumference is 25 seconds. Fig. 9 shows the measurement result of 4 roundness measurements of the barrel with 4 inner steps. All 4 measurement results indicate less than 0.8 μm, showing good roundness. In addition, this measurement setting can calculate the diameter upon circumference measurement as the rotation center of the AZ axis is obtained prior to the measurement. Hence, the diameter value is automatically acquired when measuring circumferences. Table 1 shows the 20-time repeated measurement result of the diameter and the center position of the barrel, having 3.0 mm diameter, under ±0.5 °C environment. Since diameter values are sensitive to temperature fluctuations, PV value of the diameter shows relatively large value of 0.4 μm, whereas that of the central coordinate is 0.06 μm, indicating a stable value. Fig. 10 shows the eccentricity of 7 circumferences after leveling the measurement data by the center points of point 7 at the top and point 1 at the bottom. The eccentricity amount changes in an elliptic form, however all the eccentricity values fall within 0.3 μm.

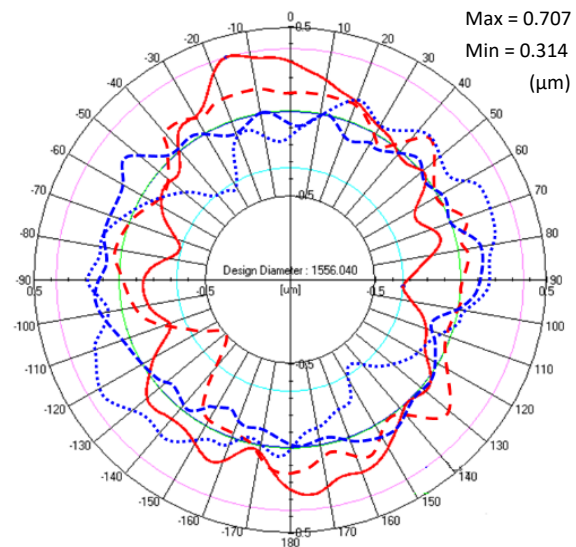


Figure 9. Roundness of four inner circumferences

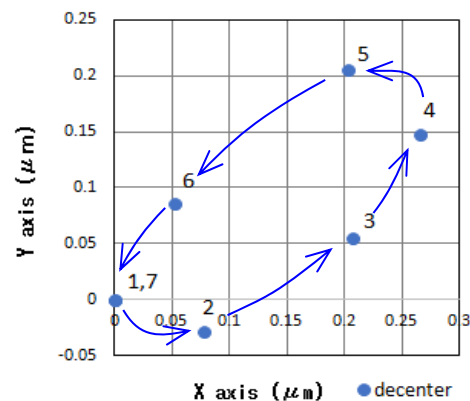


Figure 10. Eccentricity of seven circumferences

**Table 1** Diameter and center position repeatability

Item	Diameter	X	Y
MAX	3003.03	1.82	1.35
MIN	3002.65	1.78	1.30
PV	0.38	0.04	0.06
STDEV	0.12	0.01	0.02
AVERAGE	3002.78	1.80	1.32

**4.4. Measurement example 3): 3D form measurement**

Fig. 11 shows the 3D CAD comparison of 3D inner form measurement of a barrel having 6 mm diameter, 4.1 mm depth and 6 inner steps. The Z axis was set as the stepping axis and the scanning speed of the AZ axis was set at 60° per second with Scan mode. Sampling pitch in the Z axis is 20 μm and that of the AZ axis is 0.1°. The total measured points are 740,000 points and the measurement time is 38 minutes. The form deviation is expressed in color. The upper area shows approximately 8 μm of quadrate shape deviation. This is caused by sinking in injection molding, having the quadrate flange at the top of the barrel. In this way, 3D data offer surface information visually that is useful for root cause analysis of the form deviation.

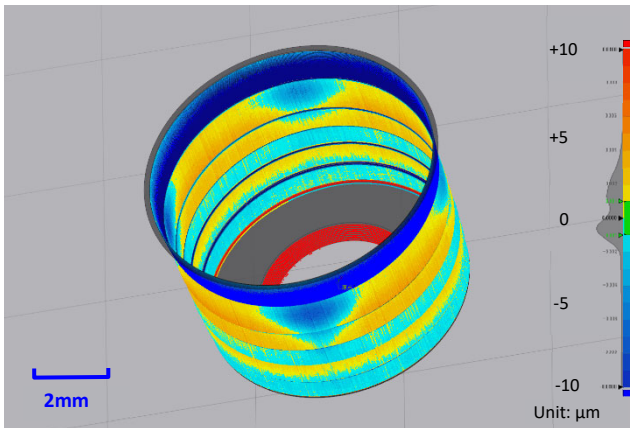


**Figure 11.** 3D form deviation of barrel inner surface

**5. Inner circumference measurement of minute hand of watch**

As an example of measuring small precision parts, the inner circumference of center hole of the wristwatch minute hand was measured. Fig. 12 shows the inner circumference measurement with the 100x objective. The angle of the AF axis was set at 75° where the objective will not be in contact with the flat plane. Fig. 13 shows the measurement result of inner surface with 0.7-mm diameter and 0.4-mm depth in 3D form. The color bar indicates the form deviation against the design values. The red indicates +1 μm and the blue indicates -2 μm. Even though this hole is produced by precision press processing, its roundness is within 3 μm. Also, the result clearly shows the 3D surface texture of the inner surface which was well obtained by AFOT.

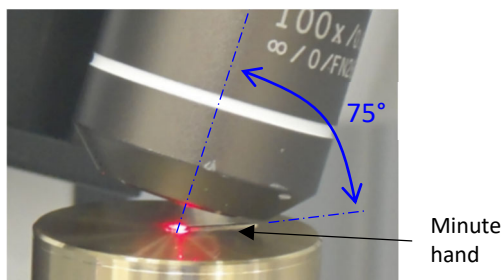


**Figure 12.** Center hole measurement of a minute hand

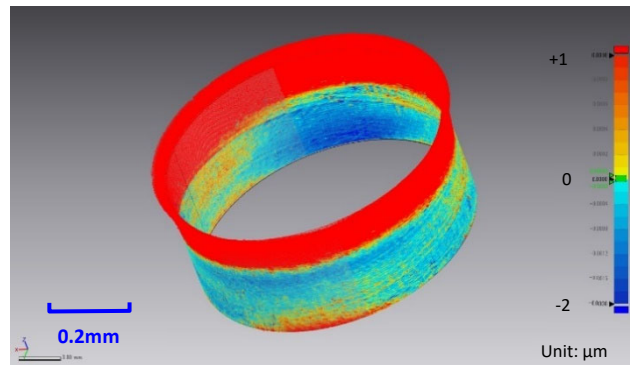


**Figure 13.** 3D measurement center hole with D = 0.7 mm

**6. Summary**

AFOT offers direct and high precision measurement of inner surface and circumference of small complex parts whose diameters are less than several millimeters.

The findings of this study are as follows:

1. Since measurement accuracy of the AF axis at the inclination angle deteriorates near the maximum measurable inclination angle ( $A_3$ ), it is effective to set the AFOT angle greater than  $A_3$  where only the scattered light is used for the measurement. The best tilt angle is 45° with the 50x objective and 60° with the 100x objective for the inclined planes having sub-micron roughness that generates scattering light.
2. The 50x objective with working distance = 10.6 mm can measure inner diameters having 7 mm with its depth up to 7 mm with AFOT.
3. The measurement repeatability of the roundness is less than 0.1 μm from the result of the 20-time repeated measurement of the 2 ring gauges.
4. Diameter measurement is sensitive to environmental temperature.
5. Only by changing the scanning axis and the stepping axis of PAP, it is possible to carry out inner cross-section contour, diameter, roundness, eccentricity and 3D form measurements of each inner step of the barrel without replacing it.

AFOT is ideal for inner circumference measurement of small complex parts such as lens barrels for smartphones, which none of the conventional measuring methods have not achieved yet. AFOT will be widely accepted in precision processing filed as the current small complex and precision parts will become even smaller in the near future.

**References**

- [1] ISO 25178-605:2014, *Nominal characteristics of non-contact (point autofocus probe) instruments*, Annex A
- [2] Miura K, Nose A, Suzuki H, Okada M, 2016 Development of cutting tool edge measurement with a point autofocus probe, *Proceedings of the 16<sup>th</sup> international conference of the euspen*, 3-4
- [3] ISO 25178-605:2014, *Nominal characteristics of non-contact (point autofocus probe) instruments*, Annex C
- [4] ISO 25178-602:2010, *Nominal characteristics of non-contact (confocal chromatic probe) instrument*, 3.4.14. Maximum acceptable local slope
- [5] Miura K, Nose A, Suzuki H, Okada M, 2014 Development and practicality of a scanning point autofocus instrument for high speed areal surface texture measurement, *Advanced Material Research*, 1017 675-680